Intense molecular emissions in the region of 431 nm in long-pulsed, electron-beam-generated helium plasmas and afterglows

L. W. Downes, S. D. Marcum, and W. E. Wells
Department of Physics, Miami University, Oxford, Ohio 45056
(Received 16 August 1985; revised manuscript received 6 March 1986)

Using an electron beam (250 kV, 200 A, 900 ns maximum pulse length) to excite ultrapure helium at a pressure of 1000 Torr, we have observed previously unreported emissions near 431 nm. These intense emissions are molecular in nature (both Q and R branches are resolvable) and have very slow rise and decay times relative to the rise and fall times of the electron-beam current pulse. A rotational constant derived from those emissions indicates that they do not originate from something other than a helium molecular species.

I. INTRODUCTION

In spite of the large number of experimental and theoretical studies that have been done to investigate the detailed nature of pure helium plasmas and afterglows, there still remains a number of problem areas in the understanding of this rather complex system. Pure helium plasmas have been examined extensively at high pressures (200—3500 Torr) using short-pulsed (3—10 ns) electron-beam excitation[1-7] and alpha particles or fission fragments,[8-12] as well as at low pressures (<100 Torr) using a variety of excitation techniques.[13-39] In recent experimental work in our laboratory, we have studied the emission characteristics of similar plasmas excited by an electron-beam generator having a variable pulse length and have found several new and important characteristics[40,41] of pure helium plasmas that were not observed during the earlier work. In our studies, time-resolved spectroscopy shows that the emission characteristics of such plasmas, while agreeing with the earlier studies at short pulse lengths, deviate considerably as the pulse length is increased. Most prominent among the newly observed phenomena is the intense emission band in the region of 431 nm that becomes, at late times in long-pulsed (>300 ns), high-pressure, electron-beam-discharge plasmas, the dominant emission characteristic of the plasma. At 1000 Torr the 431-nm emission band has a very slow risetime (>100 ns) and becomes the dominant emission feature of the plasma both at late times during the discharge as well as throughout the afterglow period. At that pressure the decay lifetime of the 431-nm emission band is approximately 2 μs.

II. EXPERIMENTAL SYSTEM

In our studies we use a variable-pulse-length (120—900 ns) electron beam to excite pure helium at 1000 Torr. The electron-beam generator produces a 10-A/cm^2 beam at 250 kV through a 2×10 cm titanium foil. The e-beam pulse is diverted to ground (having an approximately 10 ns fall time) after a length of time that depends on the number of stages (60 ns/stage, maximum of 15 stages) included in a high-voltage variable delay line. Thus, the total energy deposited in the gas is proportional to the pulse length. Fast diversion of the electron-beam pulse allows observation of a primary-excitation-free afterglow as well as the discharge period.

The detection system consists of a $\frac{1}{4}$-meter Jarrel Ash scanning spectrometer (100 μm slits) coupled to a 14-stage photomultiplier (RCA 7265) via a 10 meter length of 1-mm-diameter fused silica fiber. The fiber-optic cable was used to route the wavelength selected optical signal from the exit slit of the monochromator into a Faraday cage that houses the detection system electronics. This arrangement very significantly reduces the radio frequency interference (RFI) and x-ray noise that would be detected by the photomultiplier tube (PMT) if it were coupled directly to the monochromator. The PMT signal is digitized by a 20 MHz transient recorder and transferred to a microcomputer for storage and analysis. Figure 1 shows the overall experimental setup used for emission spectroscopy and a block diagram of the detection system elec-

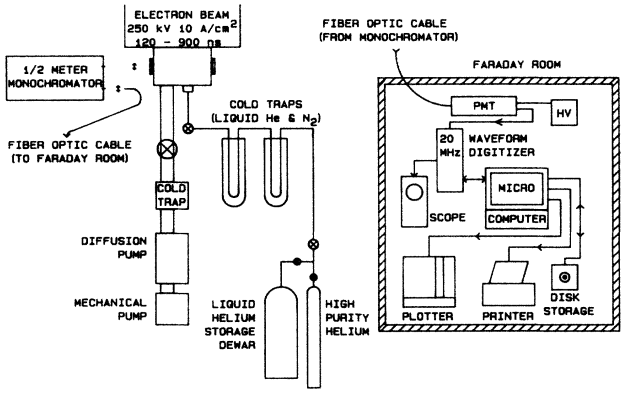

FIG. 1. Experimental apparatus used for emission spectroscopy of high-pressure, electron-beam-generated plasmas. Also shown is a block diagram of the detection-system electronics. All detection-system electronics, including the photomultiplier tube, are housed in a Faraday cage in order to reduce radio-frequency interference generated by discharges of the electron beam.

tronics. Due to the very high degree of reproducibility of the *e*-beam output, pulse-to-pulse comparisons of the emission data are straightforward. To record time- and wavelength-resolved scans of the emission spectra, the electron beam can be repetitively pulsed at up to $\frac{1}{5}$ Hz while the spectrometer can scan as slow as 0.2 nm/min. The integrated signal is displayed on the microcomputer monitor while the temporal data is stored in the memory along with that from previous pulses.

The plasma cell/gas handling system is of standard ultrahigh-vacuum (UHV) construction and has a base pressure of 5×10^{-8} Torr. Mass spectrometric analyses of the residual gases indicate that the dominant impurities are water vapor, oxygen, and nitrogen. Leak and outgassing rates are such that there is no measurable change in the residual gas pressure before the introduction of the helium. The impurity level of the helium supply is at least two orders of magnitude greater than that of the residual vacuum-system impurities even at the lowest normal operating pressure of 100 Torr. The gas handling system allows several methods of introducing high-purity helium gas into the plasma chamber. Ultrapure (99.9999%) helium can be flowed through a liquid-nitrogen trap, a combination of liquid-nitrogen and -helium traps, or liquid-helium boil-off can be used as the helium source. A schematic of the gas handling system is included in Fig. 1. With our vacuum/gas handling system we are confident that impurity levels in our gas fills are negligible. Additionally, experiments have been done using both calcium fluoride and fused silica windows on the plasma cell with no observable change in the emissions in the region of most interest in this study. For these and other reasons discussed below, we are confident that the emission signals are *not* due to either impurities or fluorescence of the plasma cell windows.

III. EMISSION RESULTS

In order to survey the helium emission spectrum, a scan was done over the range 380—650 nm and is shown in Fig. 2. The excitation pulse duration used for that scan was 900 ns and the helium pressure was 1000 Torr. Data of this type are gained by the aforementioned procedure of repetitively pulsing the electron beam while the spec-

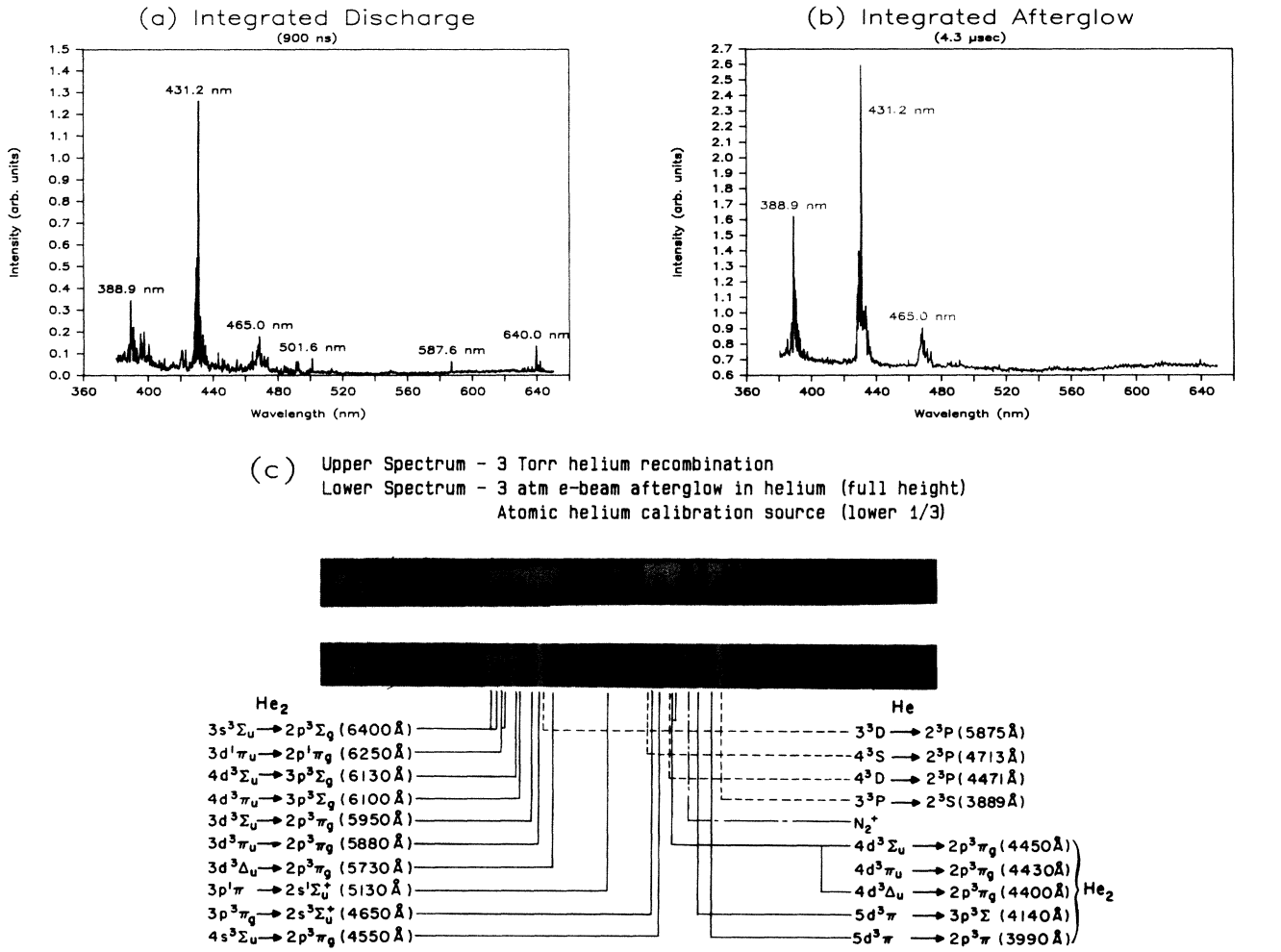

FIG. 2. Integrated emission spectra over the range 380—650 nm, (a) during the discharge of the electron beam (900-ns integration), and (b) during the afterglow (4.3-μs integration). (c) Integrated discharge and afterglow spectrum over a broader wavelength range and using an electron-beam pulse of 3-ns duration. Taken from the work of Collins *et al.* (Ref. 1).

trometer continuously scans. The spectrometer scanning rate used for the data of Fig. 2 gave 0.17 nm between e-beam pulses. Rather than present the data as three-dimensional plots of intensity versus wavelength versus time, for the sake of clarity, the wide wavelength scan of Fig. 2 has the data integrated over the discharge and afterglow periods. A number of atomic and molecular emissions similar to those found by Collins *et al.*[1,2] in their studies of pure helium excited by e-beam pulses of 3 ns duration are present in our data. A survey spectrum obtained by Collins's team[1] is included in Fig. 2 for comparison. The 388.9 nm emission that is characteristic of atomic helium ($3^3P \rightarrow 2^3S$) appears during the discharge and has a noticeable afterglow. Although nitrogen is expected to be the principal impurity, emissions from the $N_2^+(B^2\Sigma_u^+ \rightarrow X^2\Sigma_g^+)$ (391.4 and 427.8 nm) are not observable in this scan. The 391.4 nm band, when observed, provides a means of monitoring the He(2^3S) metastable population and lifetime during the late afterglow period of the e-beam discharge.[42] At longer wavelengths in that spectrum we find the characteristic emission of the He_2^* band at 465 nm ($3^3\Pi_g \rightarrow 2^3\Sigma_u^+$) and at the long wavelength end of the scan we observe the 501.5 nm ($3^1P \rightarrow 2^1S$) and 587.6 nm ($3^3D \rightarrow 2^3P$) emissions in atomic helium.

As is quite evident in the comparison of our results and those of Collins's group (Fig. 2), the very intense molecular emissions in the region of 431 nm that dominate both the discharge and afterglow periods of our plasmas are absent in Collins's emission spectra. An extensive survey of the literature[1–39] involving pure helium plasmas excited by a variety of experimental apparatus and covering a broad pressure range indicates that the 431-nm band reported here has heretofore gone unobserved. The first speculation as to the origin of the 431-nm band was, quite naturally, that it was due to an impurity present in our plasma cell. For several reasons we have come to reject that explanation for the origin of that emission. The survey scan presented in Fig. 2 was done using commercially available grade-6 helium that was introduced into the plasma cell without further purification. Results similar to those of Fig. 2 over a small wavelength range around 431 nm were subsequently obtained after the helium supply was introduced through a liquid-nitrogen trap and, later, through a combination of liquid-nitrogen and -helium traps. In addition, three different grade-6 helium supplies were used in the gas handling system with and without further purification steps. Even liquid-helium boil-off was used to fill the plasma cell. None of these impurity reduction steps affected either the intensity or the rise and decay times of the 431-nm emission. Many variations in gas-fill procedure were employed such as prolonged purging of the gas handling, plasma cell, and pumping systems with liquid-nitrogen and -helium trapped grade-6 helium, all without affecting the newly observed emissions in any significant way. Since the helium gas supplier's contaminant survey listed nitrogen as the dominant impurity, much attention was paid to possible nitrogen transitions[43] that could give rise to such emissions and none were found to be plausible candidates. Also, had nitrogen been present in sufficient quantities to account for the newly observed emissions, the aforementioned nitrogen indicator band at 391.4 nm would have been observable. We have even gone so far as to intentionally add nitrogen as a low-level impurity and have observed diminution rather than enhancement of the 431-nm emission. In order to test whether or not the newly observed emissions were due to contaminants liberated from the titanium foil that separates the plasma cell from the vacuum diode chamber of the electron-beam device, an aluminum foil was placed between the e-beam foil and that portion of the plasma that was viewed by the optical

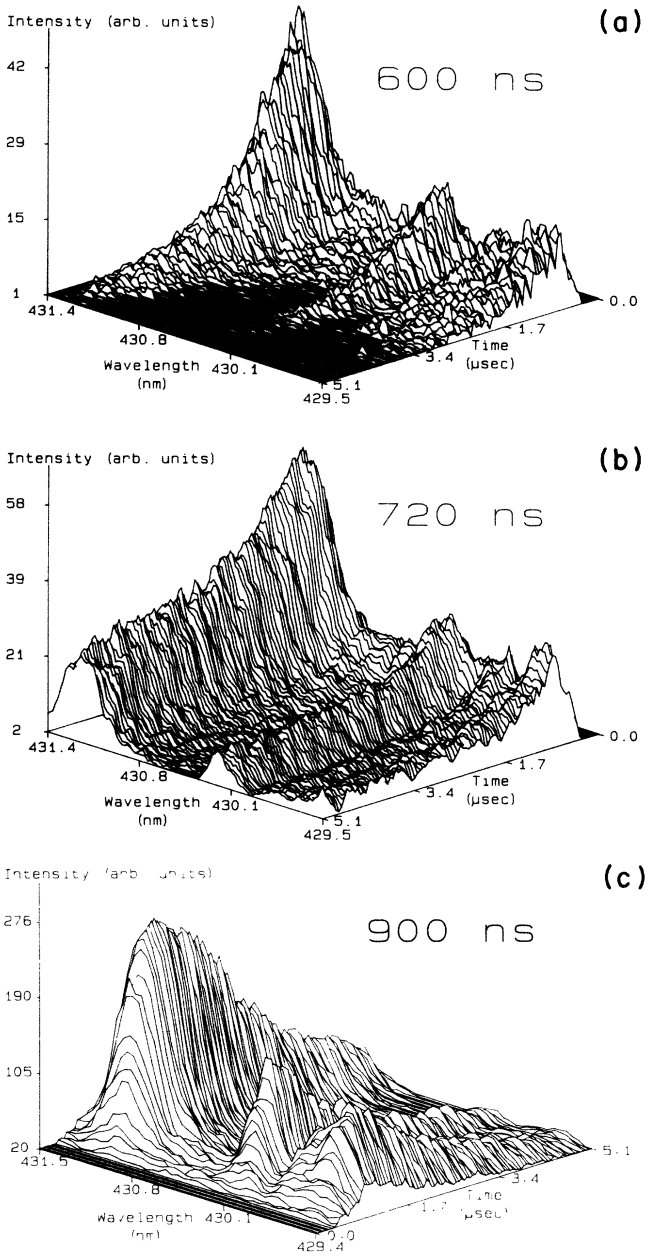

FIG. 3. Plots of intensity vs wavelength vs time in the region around 431 nm for excitation pulse lengths of 600, 720, and 900 ns. The helium pressure used in each case was 1000 Torr. The 600 and 720 ns plots have been rotated 180° to show the long afterglow lifetime, while the 900-ns plot show the slow rise time.

detection system. No appreciable change in the emission characteristics in the region of 431 nm was observed with the aluminum foil in place. It should also be noted that the 431-nm band was absent when 110 Torr of argon (having approximately the same electron-beam stopping power as 1000 Torr of helium) was used as the test gas.

Since we normally use the full 900-ns pulse of our electron beam, in order to verify the notion that the 431-nm emission was a new phenomena that could be observed only in long-pulsed *e*-beam excited, high-pressure helium plasmas, the excitation pulse length was shortened to 120 ns. This is the shortest pulse that is usable and still have sufficient energy through the foil to excite the gas. Spectral scans over a small wavelength range around 431 nm showed no significant emission above background noise for that pulse length. Only after the pulse length was increased to at least 360 ns was significant 431-nm emission observed. Plots of intensity versus wavelength versus time for the region around 431 nm using 600-, 720-, and 900-ns pulse lengths are shown in Fig. 3. As is evident from those plots, all emission bands in the region of 431 nm have slow risetimes and their decay times into the afterglow are surprisingly long. Time-resolved emission of the most intense of the 431-nm bands from an accumulation of data from 25 pulses of the electron beam is shown in Fig. 4. That data is representative of that from the satellite emissions evident in Fig. 3 and indicates that the risetime of the 431-nm emission is on the order of 100 ns. Note that the peak intensity is not reached until *after* the *e*-beam pulse is diverted to ground and that the decay time in the afterglow is on the order of 2 μs. Each point plotted in Fig. 4 represents 1 50-ns sampling period of our analog-to-digital converters. Extrapolation of the data back to a 3-ns pulse similar to that used in the studies of Collins *et al.*[1,2] indicates that the 431-nm emissions could not have been observed in their work.

In addition to monitoring the 431.2-nm emission, the atomic helium emissions at 388.9, 501.5, and 587.5 nm were also observed. The nitrogen emission (391.4 nm) was monitored both to determine the time evolution of the helium metastable population [He(2^3S)] (Ref. 42) and to have a check on the level of contamination in the plasma cell. Time-resolved emission as well as peak intensity versus excitation pulse length at those wavelengths and at 431 nm is shown in Figs. 5(a) and 5(b), respectively. In those plots, even though there is no correction for the spectral response of the system, it is again obvious that the 431-nm emission would not be observable with a 3-ns excitation pulse, and, that our data substantially agree with those of earlier studies[1–7] at early times during the *e*-beam discharge.

Close scrutiny of the risetimes of the five monitored emissions [Fig. 5(a)], shows that the atomic helium lines at 388.9, 501.5, and 587.5 nm and the 391.4-nm nitrogen emission all follow the rise of the electron-beam discharge, but the 431-nm emission is much slower. The 391.4-nm band follows the He^+ and He_2^+ populations during the discharge, while during the late afterglow it follows the metastable [He(2^3S)] population.[42] It is also apparent that the afterglow lifetime of the metastable is somewhat shorter than the 431.2-nm emission in Fig. 5(a). The helium atomic line at 388.9 nm [He($3^3P \rightarrow 2^3S$)] has an afterglow lifetime that is the same, within experimental

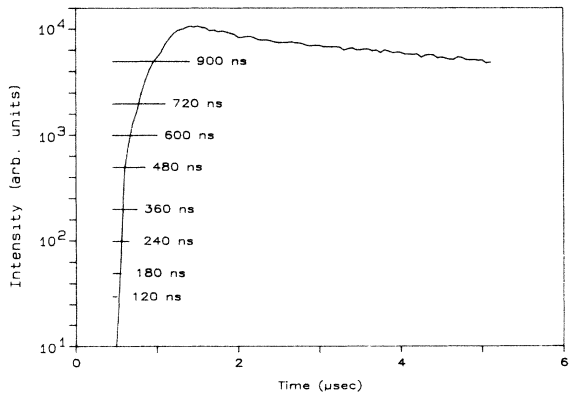

FIG. 4. Time-resolved emission of the most intense 431-nm band. The other pulse lengths used in this study are indicated on the plot. Extrapolation of the emission back to pulse lengths <50 ns indicates that the emission bands near 431 nm should not be observable for excitation pulse lengths of 3–10 ns such as those used in Refs. 1–7.

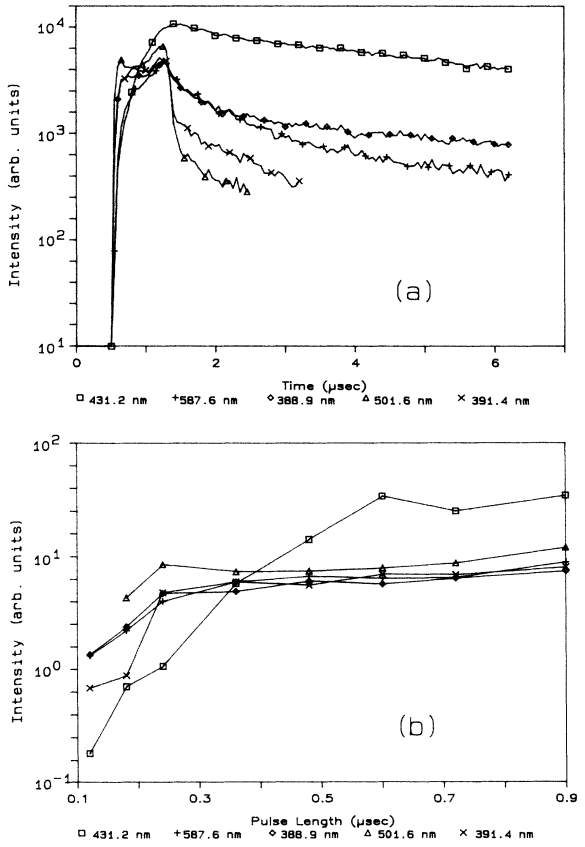

FIG. 5. (a) Time-resolved emission at 431, 388.9, 501.5, 587.5, and 391.4 nm (not corrected for relative spectral response). The symbols have been used to clarify each emission and represent every fifth point. (b) Peak intensity of 431, 388.9, 501.5, and 587.5 nm vs excitation pulse length (not corrected for relative spectral response).

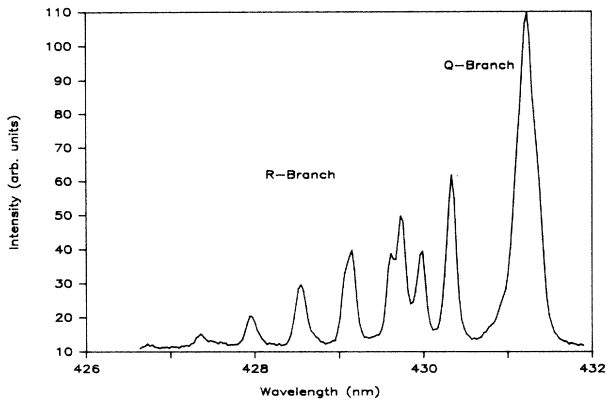

FIG. 6. Time-integrated spectrum in the region around 431 nm showing the Q and R branches of the newly observed helium emission.

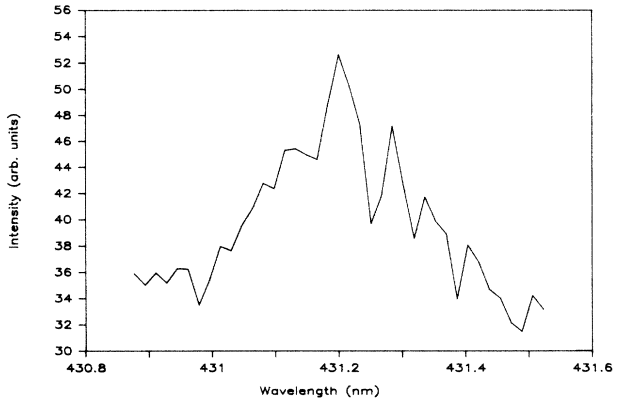

FIG. 7. Higher-resolution scan over the peak identified as the Q branch in Fig. 6. Though the individual peaks are not completely resolved, this plot suggests the closely spaced rotational structure indicative of a Q-branch-type emission

error, as that of the 431-nm emission, suggesting that the He(3^3P) state may be one of the dissociation products of whatever species is emitting the 431-nm band.

Assuming that the satellite peaks near the main 431-nm emission form the R branch of a diatomic molecular emission, we can estimate the value of the rotational constant, B_e, of the emitting species. Figure 6 shows the time-integrated spectrum in the region around 431 nm. The wavelength difference between adjacent peaks in what we identify as the R branch is measured to be 0.61 ± 0.03 nm. Assuming a complete intensity alternation for the R branch, as one would expect due to the nuclear spin of the ^{4}He atom, that spacing indicates a rotational constant of 8.3 ± 0.8 cm^{-1}. Assuming that every rotational line is present has the effect of just doubling that value for the rotational constant. Herzberg[44,45] lists an extensive set of rotational constants for a wide variety of molecules including He_2^+ ($B_e=7.2$ cm^{-1}), He_2^* ($B_e=7.06-7.77$ cm^{-1}), N_2^* ($B_e=1.07-2.01$ cm^{-1}), and N_2^+ ($B_e=1.65-2.08$ cm^{-1}). The value of the rotational constant estimated from the results shown in Fig. 6 is slightly larger than those listed[44] for He_2^* and He_2^+ and is very different from that of the most probable impurities N_2^* and N_2^+. The only other molecules listed by Herzberg[44,45] that have rotational constants similar to that measured in this study (e.g., BeH, $B_e=10.4$ cm^{-1}; HCl, $B_e=10.6$ cm^{-1}; etc.) are very unlikely to be present in the experimental system used for this study. The rotational constant that is indicated by assuming that every rotational line is present in the R branch gives similarly implausible impurities. Additionally, were such impurities the origin of the 431-nm band observed in this work they should have been detected during the optical and mass spectrometric analyses discussed above. Figure 7 shows a higher resolution (25 μm spectrometer slits instead of 100 μm) scan over the most intense of the 431-nm-band emissions. Though not quite resolved it is nevertheless apparent that there is some structure associated with that emission identified as the Q branch in Fig. 6. The satellite peaks identified as belonging to the R branch in that figure do not show any structure at the higher resolution used to obtain the data of Fig. 7.

An additional test was performed using a pulsed discharge lamp (1.5 kV, 20 μs pulse length, and 100 Torr He) coupled to the same gas handling system, helium supply and detection system used for the electron-beam studies. Although the normal emission characteristics of excited helium were present in the discharge lamp, no emissions similar to those observed in the electron-beam-generated plasmas at 100 Torr in the region of 431 nm were observed in the pulsed lamp. This test is in agreement with the results of earlier studies[30–39] performed on pure helium plasmas at low pressures that were excited by a variety of means.

IV. COMPARISON TO KNOWN He_2^* BANDS

The only helium emission bands found during our literature search that have spectral characteristics even remotely similar to those of the 431-nm band that we observe are the $He_2(I^1\Pi_g, v=0)\rightarrow He_2(A^1\Sigma_u^+, v=1)$ (Refs. 14 and 15) and $He_2(e^3\Pi_g, v=1)\rightarrow He_2(a^3\Sigma_u^+, v=0)$ (Ref. 15) transitions with peak intensity lines in the Q branch reported[15] at 431.2924 and 432.0390 nm ($\pm4\times10^{-4}$ nm), respectively. The peak intensity line we measure to be at 431.26 ± 0.03 nm. We believe that those transitions are not possible sources of the emission band reported here for several reasons. Neither the wavelengths of, nor the spacing between the various reported branch members in the above transitions agree with those measured in our work. In particular, the spacing differences are roughly a factor of 7 larger than our stated error and indicate different rotational constants for the states involved in the previously reported transitions and the one reported here. Also, the 431-nm band arises from a $v=0\rightarrow1$ transition and one would expect that the $v=0\rightarrow0$ transition[22] at 400 nm would also be easily observable in our spectra [see Figs. 2(a) and 2(b)] if an $I^1\Pi_g\rightarrow A^1\Sigma_u^+$ transition were responsible for the 431-nm band we have observed. In relation to the $v=1\rightarrow0$ band at 432 nm a similar argument can be made. The $v=0\rightarrow1$ and $1\rightarrow1$ transitions between the $e^3\Pi_g$ and $a^3\Sigma_u^+$ states at 505 and 467 nm, respectively, should also be quite intense in our spectra if the

$v=1\rightarrow 0$ transition is giving rise to the emissions we observe. We observe no evidence of intense emissions at those wavelengths or at other wavelengths in either the $\Delta v=0$ or 1 sequences of that transition in our spectra.

V. CONCLUSIONS

Having made extensive tests to determine the origin of the emission band at 431 nm we conclude that the emission results from a transition between two molecular helium levels that are as yet unidentified. The emission band is *not* due to any impurity in our plasma cell, a peculiarity of the detection system used or fluorescence of the *e*-beam cell windows. A number of areas relating to the newly identified 431-nm band need further investigation. The pressure dependence of the 431-nm emission is a current subject of study in our laboratory. The inability to observe the 431-nm band in a pulsed discharge lamp at 100 Torr, while it is easily observed in the electron-beam generated plasmas in the same gas, suggests a probable electron temperature dependence that needs further study. Additionally, preliminary results suggest that a broad band absorption (350—550 nm), having approximately the same rise and fall times as that of the 431-nm emission band, is also a characteristic of long-pulsed, electron-beam initiated plasmas and afterglows. The detailed character of this previously unreported absorption, as well as its relation to the helium species emitting the 431-nm band also need to be developed. Of course, the identity of the states involved in the emission of the 431-nm band and the details of the kinetics that describe the production and destruction of those states must also be established.

ACKNOWLEDGMENTS

This research was supported in part by the Miami University Faculty Research Committee.

[1]C. B. Collins, A. J. Cunningham, and B. W. Johnson, *Recombination Laser,* Annual Report to the U.S. Office of Naval Research, Defense Advanced Research Projects Agency (DARPA) Contract No. N00014-67-A-0310-0007, 1973 (unpublished).
[2]A. J. Cunningham, B. W. Johnson, and C. B. Collins, Phys. Lett. **45A**, 473 (1973).
[3]C. B. Collins, A. J. Cunningham, S. M. Curry, B. W. Johnson, and M. Stockton, Appl. Phys. Lett. **24**, 245 (1974).
[4]J. E. Lawler, J. W. Parker, L. W. Anderson, and W. A. Fitzsimmons, Phys. Rev. A **19**, 156 (1979).
[5]D. P. Colton, R. A. Sierra, and A. J. Cunningham, J. Phys. B **12**, 1043 (1979).
[6]J. W. Parker, L. W. Anderson, W. A. Fitzsimmons, and C. C. Lin, J. Chem. Phys. **73**, 6179 (1980).
[7]J. Stevefelt, J. M. Pouvesle, and A. Bouchoule, J. Chem. Phys. **76**, 4006 (1982).
[8]P. Harteck, S. Dondes, and P. Rentzepis, Z. Phys. **156**, 522 (1959).
[9]W. R. Bennett, Jr., Ann. Phys. **18**, 367 (1962).
[10]S. Dondes, P. Harteck, and C. Kunz, Radiat. Res. **27**, 174 (1966).
[11]J. C. Guyot, G. H. Miley, and J. T. Verdeyen, J. Appl. Phy. **42**, 5379 (1971).
[12]A. B. Callear and R. E. M. Hedges, Trans. Faraday. Soc. **66**, 2921 (1971).
[13]W. E. Curtis and R. G. Long, Proc. R. Soc. London **108**, 513 (1925).
[14]W. Weizel and Chr. Fuchtbauer, Z. Phys. **44**, 431 (1927).
[15]G. H. Dieke, T. Takamine, and T. Suga, Z. Phys. **49**, 637 (1928).
[16]W. E. Curtis and A. Harvey, Proc. R. Soc. London **121**, 381 (1928).
[17]G. H. Dieke, S. Imanishi, and T. Takamine, Z. Phys. **54**, 826 (1929).
[18]S. Imanishi, Sci. Pap. Inst. Physic. Chem. Res. (Tokyo) **10**, 193 (1929).
[19]S. Imanishi, Sci. Pap. Inst. Phys. Chem. Res. (Tokyo) **10**, 237 (1929).
[20]S. Imanishi, Sci. Pap. Inst. Phys. Chem. Res. (Tokyo) **11**, 139 (1929).
[21]W. Weizel and E. Pestel, Z. Phys. **56**, 197 (1929).
[22]G. H. Dieke, S. Imanishi, and T. Takamine, Z. Phys. **57**, 305 (1929).
[23]J. J. Hopfield, Astrophys. J. **72**, 133 (1930).
[24]W. F. Meggers and G. H. Dieke, Bur. Stand. J. Res. **9**, 121 (1932).
[25]G. H. Dieke and E. S. Robinson, Phys. Rev. **80**, 1 (1950).
[26]M. L. Ginter, J. Chem. Phys. **42**, 561 (1965).
[27]M. L. Ginter, J. Mol. Spectrosc. **17**, 224 (1965).
[28]M. L. Ginter, J. Mol. Spectrosc. **18**, 321 (1965).
[29]M. L. Ginter, J. Chem. Phys. **45**, 248 (1966).
[30]C. B. Collins and W. B. Hurt, Phys. Rev. **177**, 257 (1969).
[31]C. B. Collins and W. B. Hurt, Phys. Rev. **179**, 203 (1969).
[32]C. B. Collins, H. S. Hicks, and W. E. Wells, Phys. Rev. A **2**, 797 (1970).
[33]C. B. Collins, H. S. Hicks, W. E. Wells, and R. Burton, Phys. Rev. A **6**, 1545 (1972).
[34]J. Boulmer, J. Stevefelt, J.-F. Delpech, and J.-C. Gauthier, Phys. Rev. Lett. **30**, 199 (1973).
[35]J. Boulmer, J. Stevefelt, and J.-F. Delpech, Phys. Rev. Lett. **33**, 1248 (1974).
[36]R. Deloche, P. Monchicourt, M. Cheret, and F. Lambert, Phys. Rev. A **13**, 1140 (1976).
[37]J. Boulmer, F. Devos, J. Stevefelt, and J.-F. Delpech, Phys. Rev. A **15**, 1502 (1977).
[38]J.-F. Delpech, J. Boulmer, and F. Devos, Phys. Rev. Lett. **39**, 1400 (1977).
[39]R. Johnsen, A. Chen, and M. A. Biondi, J. Chem. Phys. **73**, 1717 (1980).
[40]L. W. Downes, S. D. Marcum, and W. E. Wells, Bull. Am. Phys. Soc. **30**, 146 (1985).
[41]L. W. Downes, S. D. Marcum, and W. E. Wells, Bull. Am. Phys. Soc. **31**, 145 (1986).
[42]T. Ueno, A. Yokoyama, S. Takao, and Y. Hatano, Chem. Phys. **45**, 261 (1980).
[43]A. Lofthus and P. H. Krupenie, J. Phys. Chem. Ref. Data **6**, 113—307 (1977).
[44]G. Herzberg, *Spectra of Diatomic Molecules* (Van Nostrand Reinhold, New York, 1950).
[45]G. Herzberg, *Electronic Spectra of Polyatomic Molecules* (Van Nostrand Reinhold, New York, 1966).

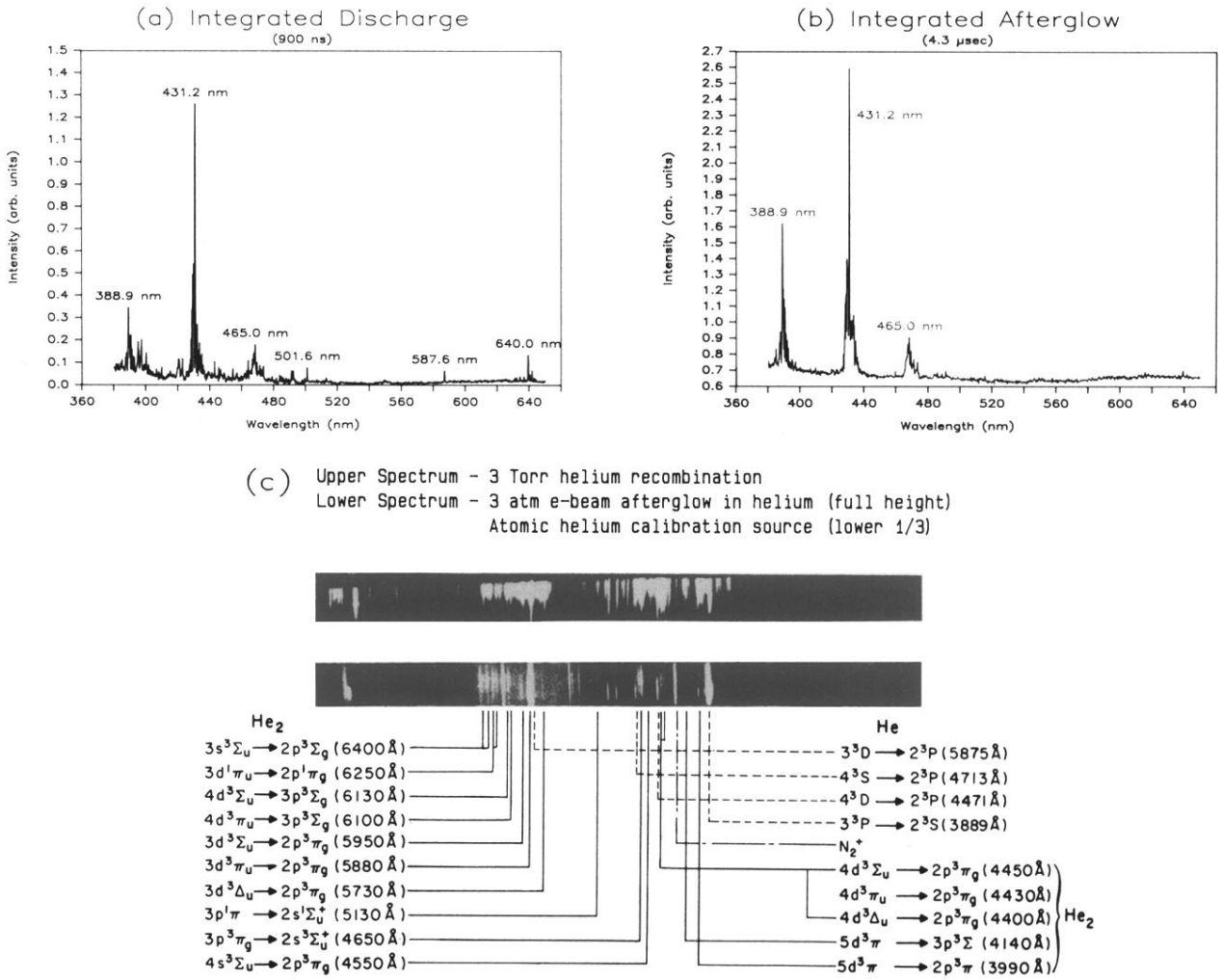

FIG. 2. Integrated emission spectra over the range 380—650 nm, (a) during the discharge of the electron beam (900-ns integration), and (b) during the afterglow (4.3-μs integration). (c) Integrated discharge and afterglow spectrum over a broader wavelength range and using an electron-beam pulse of 3-ns duration. Taken from the work of Collins *et al.* (Ref. 1).

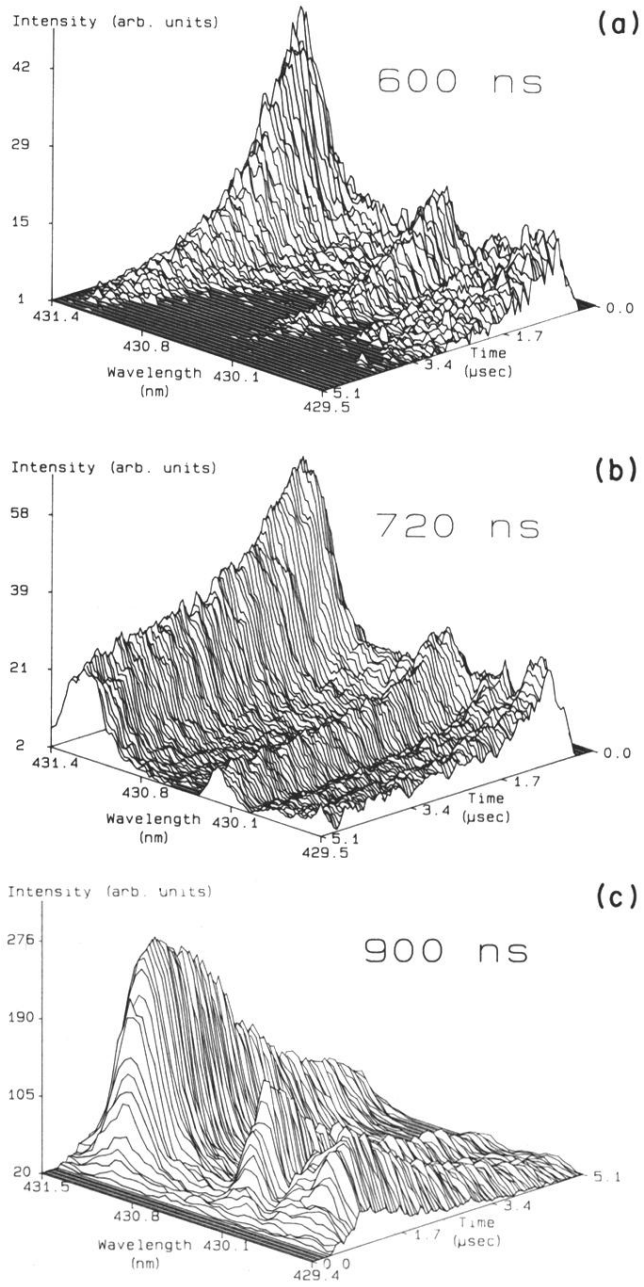

FIG. 3. Plots of intensity vs wavelength vs time in the region around 431 nm for excitation pulse lengths of 600, 720, and 900 ns. The helium pressure used in each case was 1000 Torr. The 600 and 720 ns plots have been rotated 180° to show the long afterglow lifetime, while the 900-ns plot show the slow rise time.